Band model for the electronic structure of expanded liquid mercury

L. F. Mattheiss and W. W. Warren, Jr.
Bell Laboratories, Murray Hill, New Jersey 07974
(Received 8 February 1977)

The results of a series of band-structure calculations for hypothetical forms of crystalline mercury with the fcc, bcc, sc, and diamond structures are applied to model the variation with density of $N(E_F)$, the density of states at the Fermi energy, in expanded liquid mercury. This quasicrystalline model is based on augmented-plane-wave (APW) energy-band calculations for each crystal structure with a fixed nearest-neighbor bond distance. The Fermi energy E_F and $N(E)$ for each system are derived from a tight-binding fit to the APW results along symmetry lines in the Brillouin zone. The tight-binding wave functions are applied to decompose the total $N(E)$ into its s and p components, $N_s(E)$ and $N_p(E)$, respectively. It is found that the calculated variation of $N_s(E_F)$ with coordination provides a semiquantitative explanation for the observed variation of the Knight shift in liquid mercury with density. However, the corresponding variation of $N(E_F)$ with density fails to resolve the apparent contradiction between the Knight shift and the electronic transport properties in the "strong scattering" regime.

I. INTRODUCTION

Because liquid mercury possesses a relatively low critical temperature and pressure, it can be expanded to very low densities by heating it under pressure. This has led to experimental studies of several of its physical properties as a function of density, including its electrical conductivity,[1-3] thermopower,[2,3] Hall coefficient,[4] and Knight shift.[5] Each of these properties exhibits remarkable variations with density. For example, it is found that the electrical conductivity decreases by eight orders of magnitude as the density is reduced from 13.6 to 2 g/cm^3. A comparison of these conductivity, thermopower, Hall-coefficient, and Knight-shift data leads to the conclusion that a rather gradual metal-semiconductor transition occurs in liquid Hg in the range $\rho \approx 8-9$ g/cm^3.

As is well known, this type of metal-semiconductor transition is expected at reduced densities for a divalent metal such as mercury when the $6s$ and $6p$ conduction bands no longer overlap. In the case of a liquid, the sharpness of this transition would probably be reduced by density fluctuations and the general loss of long- and short-range order.

Mott[6] has proposed an intuitive theory for liquid Hg that is based on these simple theoretical ideas. According to Mott, the band structure for a hypothetical form of crystalline Hg in which the lattice parameter is gradually increased would produce initially a minimum in $N(E)$ near E_F and ultimately a band gap. Mott suggests that the general features of this crystalline model for Hg would survive in the liquid state, with band edges and critical points smeared out by density fluctuations and the loss of long- and short-range order. Thus, Mott replaces the fundamental energy gap for crystalline Hg by a "pseudogap" or minimum in $N(E)$ at E_F in the liquid. Mott[7] proposes that when the magnitude of $N(E)$ in this "pseudogap" decreases to some critical value, the electrons in these states become localized rather than itinerant, thereby producing a metal-semiconductor transition.

An alternative model for explaining the metal-semiconductor transition in liquid Hg has been proposed by Cohen and Jortner.[8] Their model emphasizes inhomogeneities in the local density of the fluid that are caused by density fluctuations. They suggest that these fluctuations lead to the simultaneous presence of semiconducting and metallic regions within the liquid. At high mean densities, the metallic regions dominate so that metallic paths extending throughout the material are more likely. As the mean density is decreased, the volume fraction of these metallic regions also decreases. They propose that when a critical value is reached, these extended metallic channels are no longer available and the liquid becomes semiconducting.

Analysis of the properties of liquid Hg in terms of these models is complicated by an apparent inconsistency of the Knight shift and the electronic transport properties.[5] Both the Mott description and that of Cohen and Jortner contain a "strong-scattering" transport regime which applies over an intermediate range of densities between the normal liquid metal and the metal-semiconductor transition. In this regime, it is supposed that the electronic wave functions are itinerant, extending throughout the material, but that the scattering is so strong that the electron mean free path is reduced to one interatomic spacing a. This strong-scattering situation has been discussed extensively by Cohen,[9] Mott,[10] Hindley,[11] Friedman,[12] and others. The essential theoretical prediction

is that, as the density is reduced, the conductivity σ and Hall coefficient R_H vary with a parameter $X \equiv N_V(E_F)Ja^3$ according to $\sigma \propto zX^2$ and $R_H \propto z^{-2}X^{-1}$. Here $N_V(E_F)$ is the density of states per unit volume at the Fermi level, J is an interatomic transfer integral, and z is the coordination number. This behavior is consistent with the data of Even and Jortner[4] who found $R_H^{-1} \propto \sigma^{1/2}$ over a density range of roughly 9–11 g/cm^3. The conductivity varies from 300 to 3000 $(\Omega\,\mathrm{cm})^{-1}$ over this region. In contrast, however, the Knight shift is found to be independent of density over this same range. This suggests that the s component of the density of states is constant and so raises a serious challenge to the strong-scattering description unless it can be shown that the Knight shift is influenced by additional factors or, for example, that the expected decrease in $N(E_F)$ with decreasing density is compensated by an increase in fractional s character at E_F. It is therefore of considerable interest to investigate independently the expected behavior of $N(E_F)$ and $N_s(E_F)$ in liquid Hg as a function of density.

One approach to this problem is to model the electronic structure of the liquid by means of band-structure calculations for appropriate crystalline structures. The validity of this method rests on the assumption that gross features of the electronic structure are determined by the density and local arrangement of atoms and are relatively insensitive to the degree of long-range order. The small changes of the electronic properties observed for most metals on melting provide support for this assumption. Even in cases where the bands are far from the free-electron form, there may still be little change in $N(E)$ on melting, as strikingly demonstrated by the recent x-ray photoemission study of Bi by Baer and Myers.[13]

There have been several recent band-structure calculations carried out for hypothetical forms of crystalline Hg in the low-density limit. The first calculations were by Devillers and Ross,[14] who applied the pseudopotential method to calculate the energy bands for crystalline Hg with the bcc, fcc, and rhombohedral structures. For each structure, they obtained a band gap at $\rho \approx 8.5$ g/cm^3, in general agreement with the transport data. More recently, Overhof *et al.*[15] have carried out relativistic Korringa-Kohn-Rostoker (KKR) calculations for expanded fcc and simple cubic (sc) Hg. Unlike Devillers and Ross, Overhof *et al.* find that the semiconducting gap occurs at different densities for the two structures. They find that fcc Hg becomes semiconducting at $\rho = 9.3$ g/cm^3 while sc Hg remains a conductor until $\rho = 5.5$ g/cm^3. A similar dependence on crystal structure was obtained by Fritzson and Berggren,[16] who carried out pseudopotential calculations for expanded fcc, bcc, and sc Hg and found that band gaps open up at $\rho = 6.5$ g/cm^3 for fcc, 5.5 g/cm^3 for bcc, and 4 g/cm^3 for sc Hg.

A very different approach has been taken by Yonezawa *et al.*[17] who calculate $N(E)$ for the disordered liquid metal using a tight-binding self-consistent single-site approximation. These calculations also exhibit the development of an energy gap, but at densities in the range 2–4 g/cm.^{3} This is lower than the values obtained by band calculations and also less than can be inferred from optical-absorption[18] and electrical-transport data.[1-4] Thus, the band models generally tend to produce results that are in more satisfactory agreement with experiment.

The purpose of the present investigation is to apply a new quasicrystalline model to approximate the electronic properties of expanded liquid mercury. In this study, we assume that the nearest-neighbor bond distance is constant so that the density variation in expanded liquid Hg is due entirely to changes in coordination number. Although this assumption is a likely oversimplification, available data on liquid structure suggest that it is a sound first approximation. For example, x-ray studies by Waseda and Suzuki[19] on liquid Hg at low temperatures ($\rho \approx 13.6$ g/cm^3) suggest a temperature-independent nearest-neighbor bond distance of 3.07 Å and a coordination number of 10–11. Less-complete determinations of the structure factor for liquid Hg at higher temperatures by Waseda *et al.*[20] suggest the likelihood that the nearest-neighbor bond distance remains essentially unchanged and that density reductions are due primarily to a decrease in the coordination number. This would be analogous to the situation in liquid argon, where the coordination number decreases from 10 ± 2 at high densities to 4 ± 2 near the critical point with little concommitant change in nearest-neighbor distance.[21]

The present study is based on a series of augmented-plane-wave (APW) calculations for crystalline Hg with the fcc, bcc, sc, and diamond structures and a fixed nearest-neighbor bond distance of 3.07 Å. In a perfectly ordered crystal, these calculations would correspond to densities of 16.3, 15.0, 11.5, and 7.5 g/cm^3, respectively. However, it is argued that these densities are reduced by disorder, fluctuations, etc., in the liquid state for the structures having $z < 12$ so that these quasicrystalline results correspond to liquid densities of 16.3, 10.9, 8.1, and 5.4 g/cm^3, respectively.

The results of these calculations show that the Hg 6s and 6p bandwidths and their overlap are reduced systematically as the coordination number

is decreased at a fixed nearest-neighbor distance. In particular, the $6s$-$6p$ band overlap is reduced to about 0.1 eV in the tetrahedrally coordinated diamond structure. A band gap is then opened up if the nearest-neighbor bond distance is increased by about 1% to 3.10 Å. The Slater-Koster linear-combination-of-atomic-orbitals (LCAO) interpolation method[22] has been applied to fit the results of these APW calculations along symmetry lines in the Brillouin zone. Using these LCAO eigenvalues and wave functions, we have calculated accurate density-of-states curves for each structure, including their decomposition into s and p components.

The details of the present APW calculations for Hg are described in Sec. II, along with the LCAO model and its application to the density-of-states calculation. The results of these calculations are presented in Sec. III. These include $E(\vec{k})$ and $N(E)$ curves for hypothetical fcc, bcc, sc, and diamond-structured Hg. The application of these crystalline results for interpreting the electronic properties of liquid mercury is considered in Sec. IV, while Secs. V and VI contain, respectively, a brief discussion and a summary of our results and conclusions.

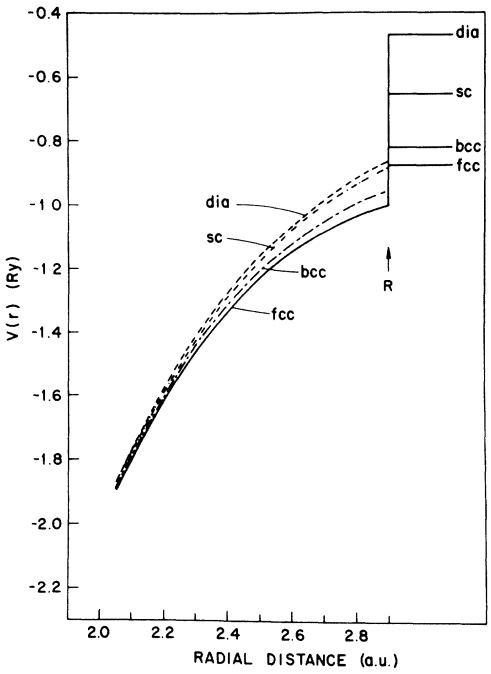

FIG. 1. Plot of the muffin-tin potentials near the APW sphere radii $R = 2.9$ a.u. for Hg with the diamond, sc, bcc, and fcc structures. Values of the average potential between the spheres are shown to the right.

II. DETAILS OF THE CALCULATIONS

A. APW calculations

The present APW calculations utilize approximate crystal potentials that are derived from overlapping relativistic Dirac-Hartree-Fock-Slater atomic charge densities[23] for Hg involving the configuration $6s^2$ and full Slater exchange ($\alpha = 1$).[24] The choice $\alpha = 1$ is often regarded as optimum for calculations in which the potential is not determined self-consistently. The present calculations have been carried out for fcc, bcc, sc, and diamond-structured Hg with a nearest-neighbor bond distance of 3.07 Å. In each case, we have included the corrections to the muffin-tin potential in the region between the APW spheres. As DeCicco has shown,[25] these warping corrections to the muffin-tin approximation are readily introduced into the APW formalism; they require the addition of one extra term to each muffin-tin APW matrix element, namely, the Fourier coefficient of the warping correction.

These corrections to the muffin-tin potential become more important as the nearest-neighbor coordination number is reduced. This is illustrated in Fig. 1, where the muffin-tin potentials near the APW sphere radius R for each crystal structure are compared. The four values for the constant potential in the interstitial regions between the APW spheres are shown to the right. The discontinuity in the potential at R varies from 0.13 Ry in the close-packed fcc structure to 0.39 Ry for the diamond structure. In each case, the APW sphere radius is 2.9 a.u. or half the nearest-neighbor bond distance.

Because of its large atomic number ($Z = 80$), relativistic effects are expected to be important for Hg in calculations dealing with the atomic, liquid, or solid state. This is evident from the relativistic APW results for rhombohedral crystalline Hg by Keeton and Loucks[26] and the perturbation-theory atomic estimates by Herman and Skillman.[27] According to Herman and Skillman, the combined effect of the Darwin and mass-velocity corrections is to lower the atomic $6s$ level of mercury by about 0.15 Ry relative to the energy of the $6p$ state. It is clear that these relativistic effects are an essential ingredient in any theoretical model for the metal-semiconductor transition in liquid Hg.

By comparison, the effects caused by spin-orbit coupling are considerably smaller than these Darwin and mass-velocity corrections. For example, an extrapolation of the Herman-Skillman results for Pb and Po suggest that the Hg $6p$ spin-orbit parameter $\xi_{6p} \approx 0.02$ Ry. As is well known, the principal effect of spin-orbit coupling on the energy-band states in solids is that of reducing the spatial degeneracy of states with wave vectors at symmetry

points and along symmetry lines of the Brillouin zone by causing splittings which are proportional to ξ.

In the present investigation, the bulk of the energy-band results have been obtained using a "partially relativistic" APW method[28] in which the Darwin and mass-velocity corrections are taken into account but spin-orbit effects are neglected. In addition, limited calculations were carried out using the fully relativistic-APW (RAPW) method.[29] A comparison between these partially and fully RAPW results allows one to study the way in which the partially relativistic bands are changed by spin-orbit coupling. In each structure, it is found that the bands near the Fermi energy E_F are spatially nondegenerate. As a result, the energies of these states were only slightly altered by the effects of spin-orbit coupling. Therefore, it is concluded that, for the purposes of the present study, spin-orbit effects can be safely neglected.

This is not the case for the Hg $5d$ bands. In their relativistic calculation for rhombohedral Hg, Keeton and Loucks[26] find that the Hg $5d$ bands are located about 8 eV below E_F, near the bottom of the $6s$-$6p$ conduction band. The relativistic KKR results of Overhof *et al.*[15] for expanded fcc and sc Hg place the $5d$ bands slightly below the bottom of the $6s$-$6p$ conduction band. In both calculations, it is clear that the $5d$ spin-orbit parameter ξ_{5d} $\approx$0.06 Ry is comparable with the $5d$ bandwidth so that spin-orbit effects are essential in an accurate treatment of these states. Similar results are obtained in the present investigation. It is found that the Hg $5d$ bands fall slightly below the bottom of the $6s$-$6p$ conduction bands in the diamond structure. These $5d$ bands gradually overlap the bottom of $6s$-$6p$ band as the nearest-neighbor coordination number increases. In the fcc structure, the position of the $5d$ bands relative to the $6s$-$6p$ bands is comparable to that obtained by Keeton and Loucks for rhombohedral Hg.

B. LCAO model

The Slater-Koster LCAO interpolation method[22] has been applied to fit the results of APW calculations along symmetry lines in the Brillouin zone for each crystal structure. For simplicity, this LCAO model has included only the Hg $6s$-$6p$ conduction bands and neglected the $5d$ bands. This leads to a 4×4 matrix for the sc, bcc, and fcc structures and an 8×8 LCAO matrix for the diamond structure, where there are two Hg atoms per cell.

In most cases, the LCAO matrix elements are obtained directly from the tables published by Slater and Koster.[22] We have included up to third-neighbor interaction parameters in our LCAO matrix. For the diamond structure, these are obtained from the work of G. Dresselhaus and M. S. Dresselhaus[30] and Alstrup and Johansen,[31] who also correct some misprints in the Slater-Koster tables.

The LCAO parameters were determined by a nonlinear-least-squares fitting procedure that has been described previously.[32] A slight modification of this procedure was introduced in the present investigation in order to simplify its application. Namely, instead of reducing the LCAO matrices at the various symmetry points by hand into their irreducible components, the proper matching of LCAO eigenvalues ϵ_i with the appropriate first-principles energy E_i was achieved within the computer codes by examining the symmetry of the LCAO eigenvectors.

The number of LCAO parameters included in this fitting procedure ranged from 16 for the fcc structure to 22 for the diamond structure. These parameters were treated in their most general form and did not involve the two-center approximation. Nearest-neighbor overlap of the $6s$-$6p$ orbitals was treated explicitly in this LCAO model. These overlap parameters were particularly effective in improving the accuracy of the fit along symmetry lines where s-p hybridization is important.

In those cases where bands originating from the more highly excited atomic states of Hg overlapped the $6s$-$6p$ manifold, it was useful to assign these upper bands a reduced weight in the LCAO fitting procedure. This helped to improve the overall accuracy in the more important energy range near E_F.

The results of Table I summarize the details of the LCAO interpolation scheme and its application to each of the four crystal structures. For each structure, the LCAO parameters were determined by fitting APW results at a uniformly spaced set of mesh points such that the Δ or $\langle 100\rangle$ axis of the Brillouin zone was subdivided into either four (sc) or eight (diamond, bcc, fcc) intervals. This provided roughly 100 band energies/atom in the unit cell for each structure. The rms error in the fit, including the reduced weighting of the upper

TABLE I. Summary of the LCAO fit to the Hg $6s$–$6p$ bands.

	Structure			
	Diamond	sc	bcc	fcc
No. of LCAO parameters	22	18	19	16
No. of wave vectors $\vec{k}_i$	27	22	26	27
No. of energies $E_n(\vec{k}_i)$	216	88	104	108
rms error (Ry)	0.008	0.009	0.014	0.017

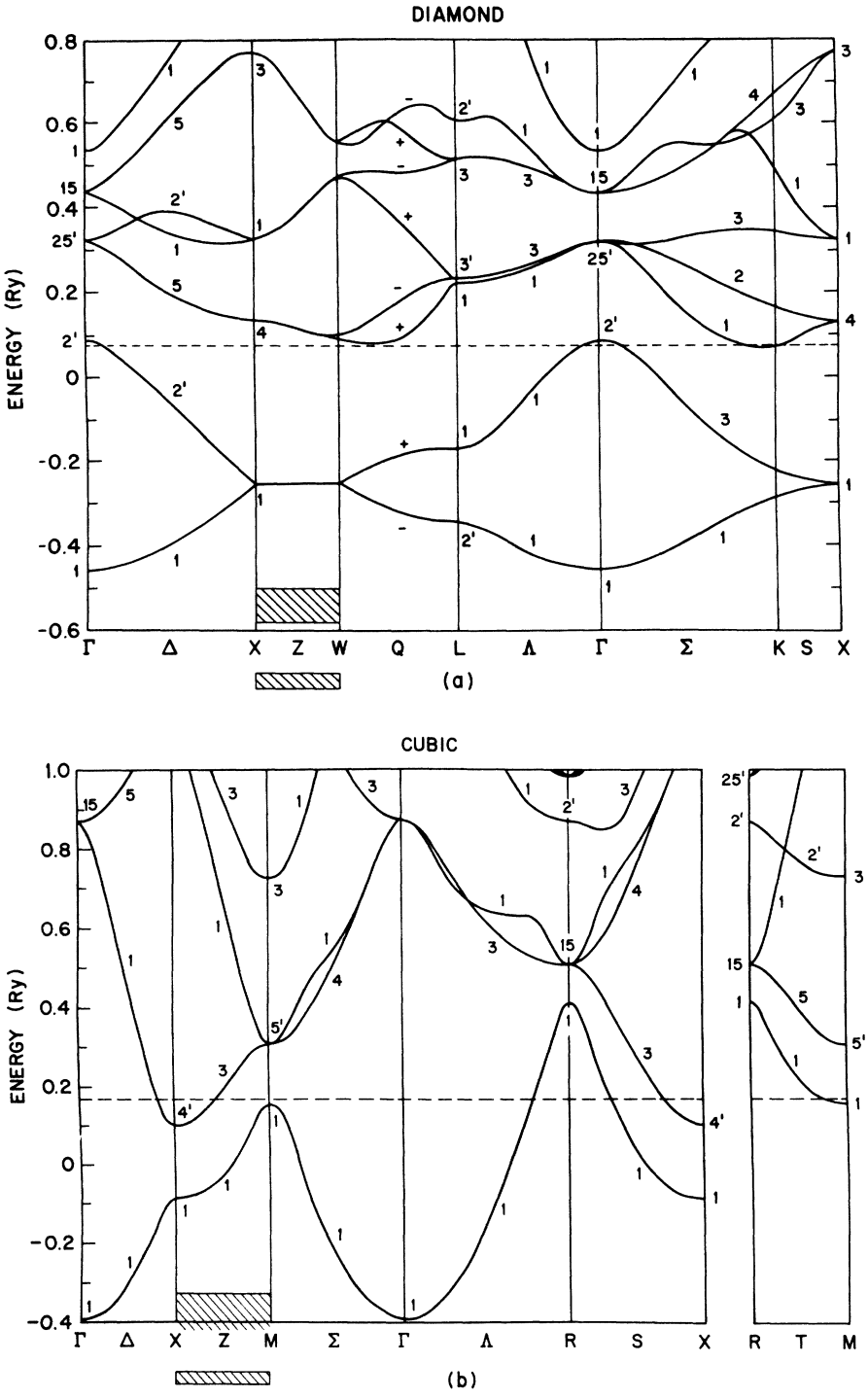

FIG. 2. APW results for hypothetical Hg with the (a) diamond, (b) sc, (c) bcc, and (d) fcc structures. The cross hatching indicates the approximate energy range of the 5*d* core states.

unoccupied bands, ranged from 0.01–0.02 Ry.

The LCAO band structures for each of these crystalline forms of Hg have been applied to determine the corresponding density-of-states curves $N(E)$ using the tetrahedral method.[33,34] This approach subdivides the Brillouin zone into tetrahedra, within which $E(\vec{k})$ is assumed to vary linearly. The values of $E(\vec{k})$ at each of the vertices determine the coefficients in simple analytic expressions for the density-of-states contribution from each band.

In the present application of this method, we have

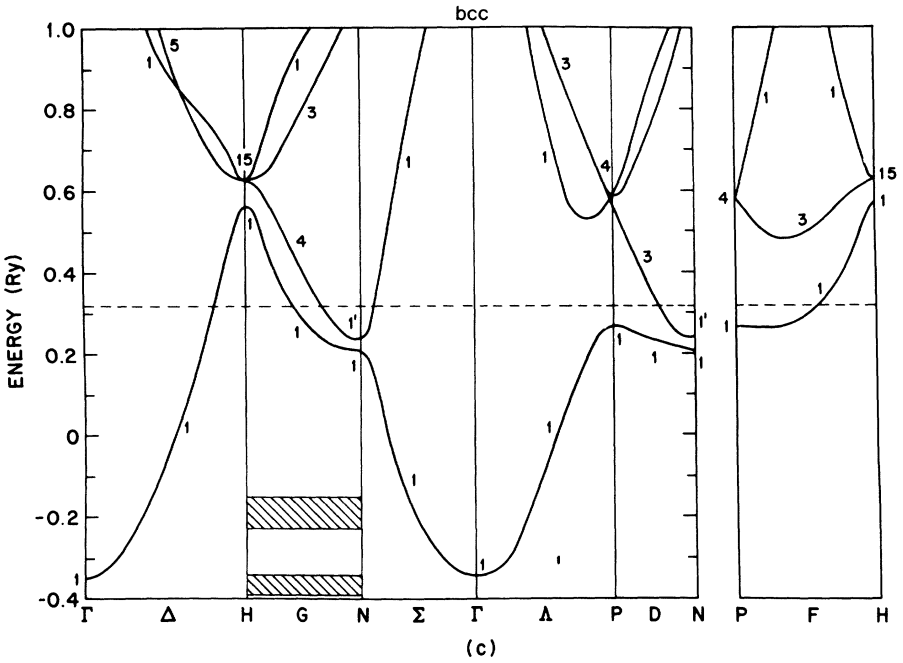

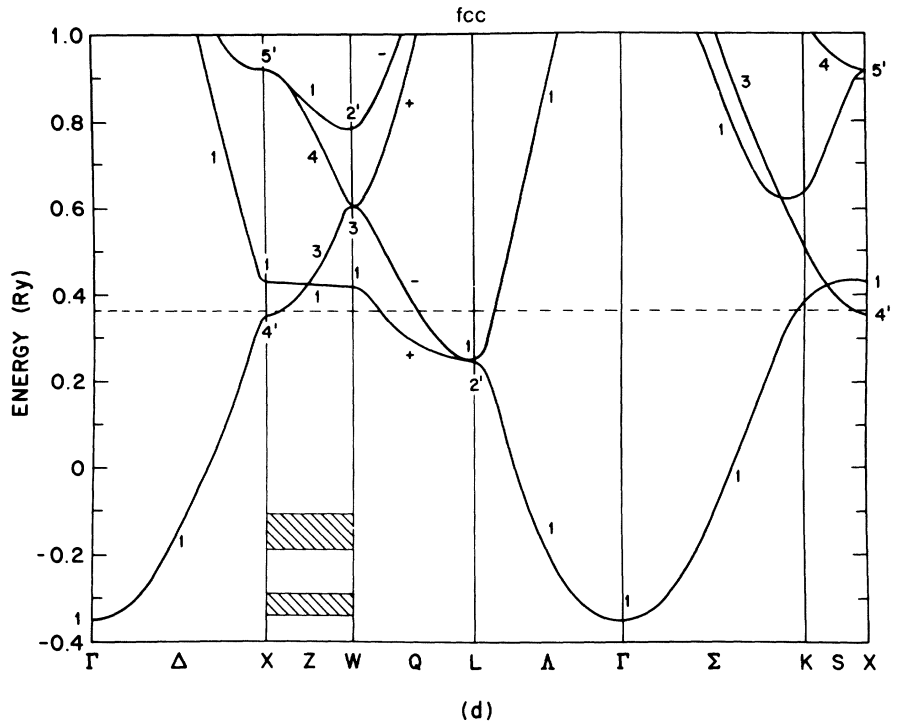

Figure 2 (*continued*)

included approximately 4000 tetrahedra within $\frac{1}{48}$ of the Brillouin zone. A comparison of these results with those obtained using half as many tetrahedra yield negligible changes in the details of $N(E)$ curves.

In addition to determining the total density of states $N(E)$, we have also determined its 6*s* and 6*p* components, $N_s(E)$ and $N_p(E)$, respectively. This involves the weighting of each contribution to $N(E)$ by the average *s* and *p* character of the LCAO wave functions at the four vertices of the tetrahedron.

III. RESULTS

The results of the "partially relativistic" APW calculations for each of the four hypothetical crystalline phases of Hg are shown in Fig. 2. In each case, the zero of energy corresponds to the average value of the potential in the region between the APW spheres (Fig. 1). The Fermi energy E_F is indicated by the dashed horizontal lines. The approximate positions of the $5d\,j=\frac{5}{2}$ and $j=\frac{3}{2}$ core levels are indicated by the cross-hatched areas along the Z and G symmetry lines of the Brillouin zone. These were determined by means of limited RAPW calculations for each structure.

The lowest pair of bands in Fig. 2(a) involve primarily the Hg 6s orbitals. At each point in the zone, these bands are about 0.2 Ry lower in energy than the lowest 6p bands. However, it is found

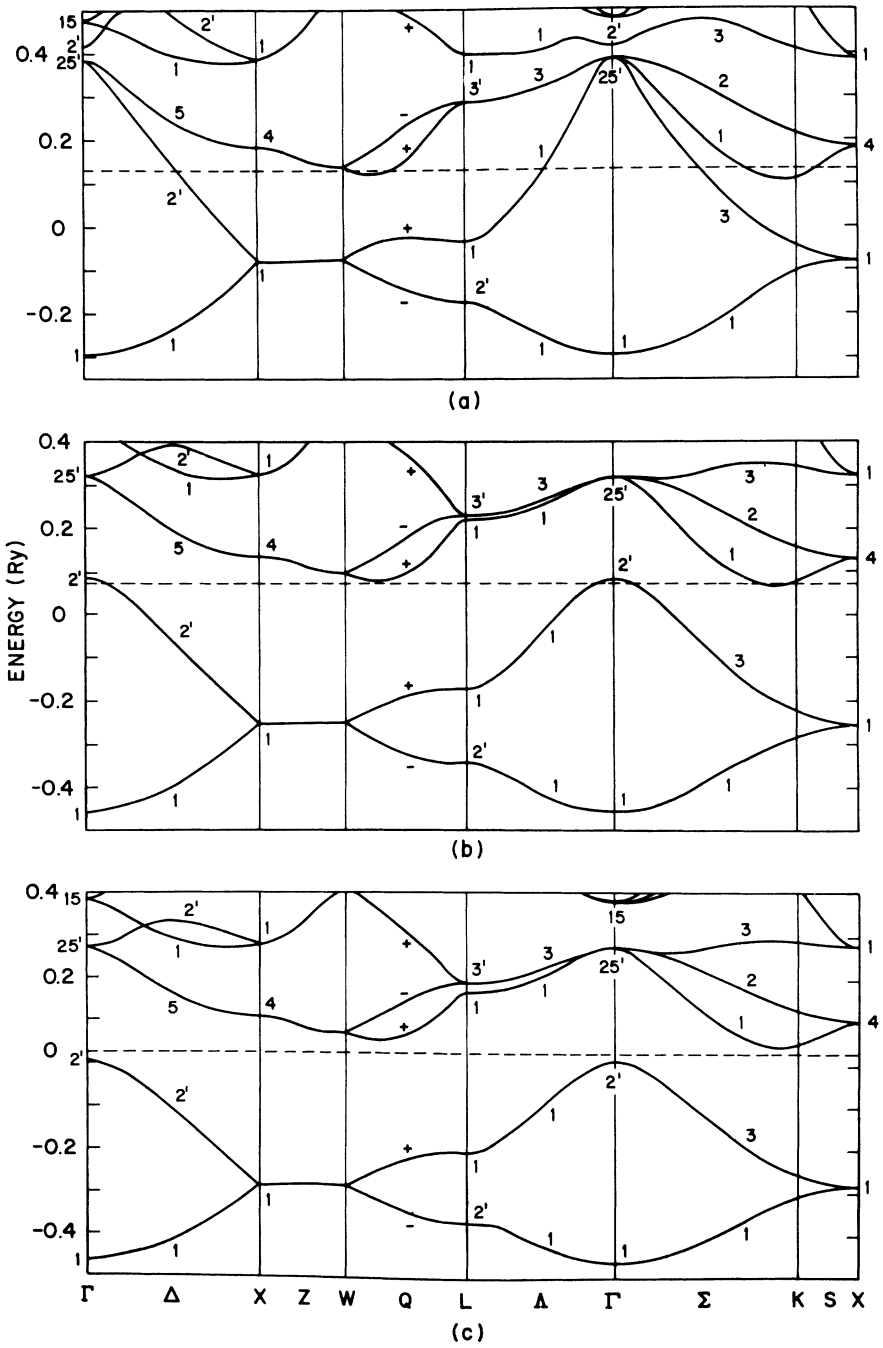

FIG. 3. Comparison of (a) nonrelativistic and (b) partially relativistic energy-band results for Hg with the diamond structure. (c) Results of a partially relativistic calculation with the lattice parameter expanded by 3.3%.

that the top of the 6s valence band ($\Gamma_{2'}$) slightly overlaps the lowest conduction-band state (Σ_1), thereby predicting semimetallic behavior. This 6s-6p band overlap gradually increases as the coordination is increased from 4 to 6, 8, and 12 in Figs. 2(b), 2(c), and 2(d), respectively. This leads to metallic behavior in the closer-packed structures. It is also clear that the bands become more nearly "free-electron"-like as the coordination is increased.

This transition from fairly narrow tight-binding bands in Fig. 2(a) to broad nearly free-electron-like bands in Fig. 2(d) is reflected in the accuracy of the LCAO fit to these bands, as summarized in Table I. It was noted in Sec. II B that this LCAO model neglected some of the higher-lying bands that evolve from excited atomic states. Some examples of these are the bands originating from the upper Γ_1 state in Fig. 2(a) as well as the M_3 and $R_{2'}$ states in Fig. 2(b).

To illustrate the importance of relativistic effects (Darwin and mass-velocity corrections) on these results, we compare in Figs. 3(a) and 3(b) the nonrelativistic and partially relativistic band

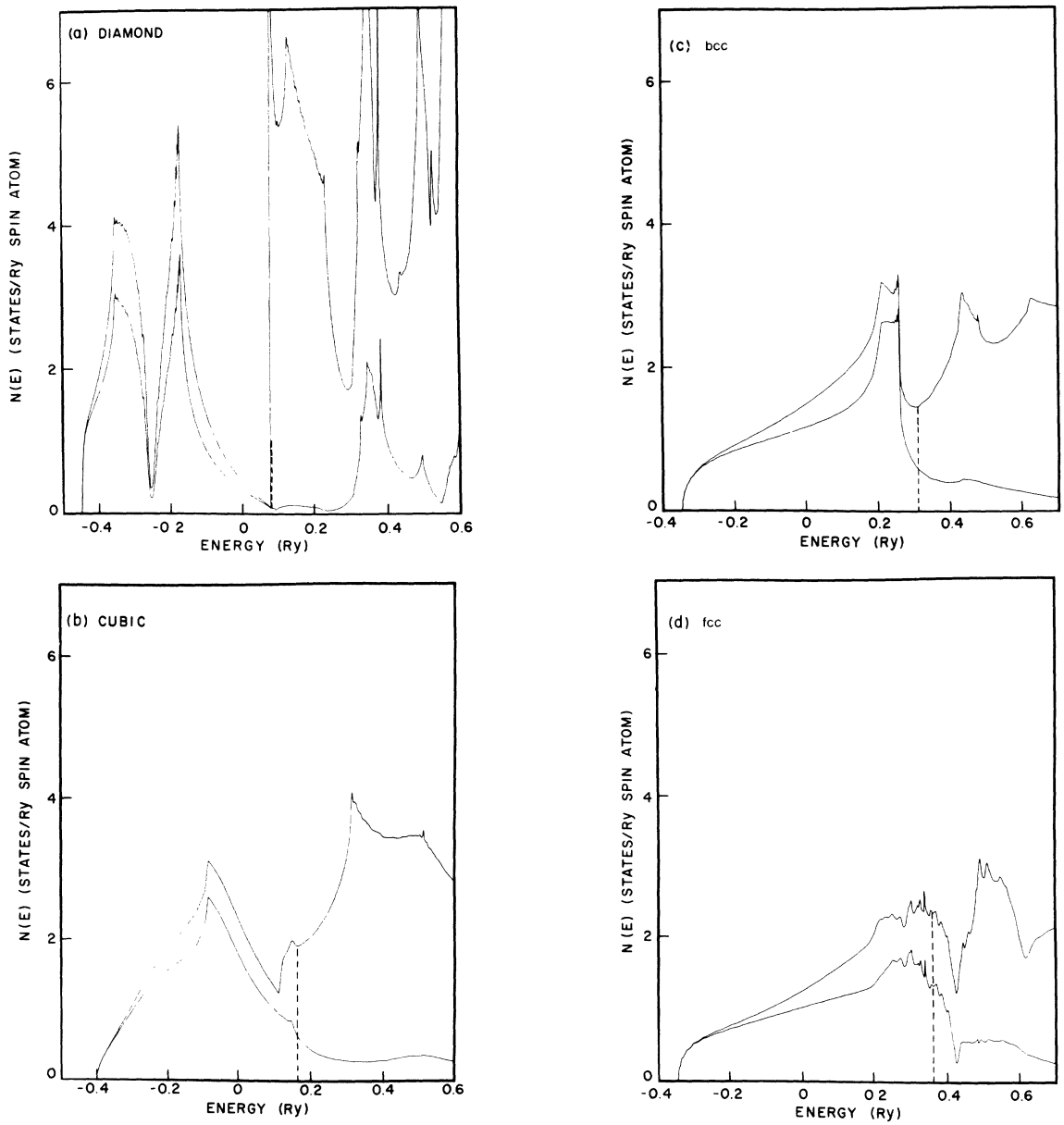

FIG. 4. Plot of $N(E)$ and $N_s(E)$ curves (upper and lower lines, respectively) as a function of energy for each crystal structure.

structures for tetrahedrally coordinated Hg. The results in Fig. 3(a) have been determined from a completely independent APW calculation involving a charge density derived from the nonrelativistic Herman-Skillman program.[27] Equivalent results are obtained if one sets the velocity of light $c = \infty$ in the partially relativistic calculations of Fig. 3(b). The ordering of levels in Fig. 3(a) is similar to that usually found in calculations for group-IV elements with the diamond structure, where a semiconducting gap separates the fourth and fifth bands.

The slight overlap of the $6s$-$6p$ bands in Fig. 3(b) disappears in Fig. 3(c) when the lattice constant is increased by 3.3%. Assuming a linear variation, it is estimated that this band overlap is zero for tetrahedral coordination when the nearest-neighbor bond distance is increased by 1% from 3.07 to 3.10 Å.

The density of states $N(E)$ has been calculated for each structure, using an LCAO interpolation of the results shown in Fig. 2. The lower energy portions of these $N(E)$ curves are shown in Fig. 4. In each case, the upper curve corresponds to the total density of states $N(E)$ while the lower one represents the $6s$ component, $N_s(E)$. The difference between the two curves is, of course, the $6p$ contribution, $N_p(E)$. The appropriate Fermi energies E_F are indicated by the dashed vertical lines.

In the case of the diamond structure, E_F falls very near the lower edge of a very sharp peak in $N_p(E)$ that is due to the conduction-band minima along Σ and Q (Fig. 2). The values of $N_s(E_F)$, $N_p(E_F)$, and $N(E_F)$ for each structure are summarized in Table II. It is found that the value of $N_p(E_F)$ is roughly constant for each structure so that the variations in $N(E_F)$ are determined primarily by the $N_s(E_F)$ contributions. These are small (~0.09) for the diamond structure, intermediate and constant (~0.56) for the sc and bcc structures, and significantly larger (~1.26) for the close-packed fcc structure.

TABLE II. Summary of density-of states results [states/(Ry spin atom)] at E_F for Hg as a function of crystal structure. The quantity g is defined as the ratio of $N(E_F)$ to the free-electron value $N_{fe}(E_F)$.

Structure	E_F(Ry)	$N_s(E_F)$	$N_p(E_F)$	$N(E_F)$	g
Diamond	0.076	0.088	0.984	1.072	0.242
sc	0.169	0.579	1.342	1.921	0.578
bcc	0.319	0.555	0.936	1.491	0.534
fcc	0.367	1.256	0.997	2.253	0.854

IV. APPLICATION TO LIQUID MERCURY

A. Structural model for expanded liquid mercury

As is well known, experimental knowledge of the structure of monatomic liquids is represented by the static liquid structure factor $S(k)$ which can be measured by x-ray or neutron diffraction. The structure factor is related by Fourier inversion to the pair distribution function $g(r)$,

$$S(k) = 1 + \int_0^\infty 4\pi r^2 n_0 [g(r) - 1] \frac{\sin kr}{kr}\, dr, \qquad (1)$$

where n_0 is the number density. The radial distribution function $n(r) \equiv 4\pi r^2 n_0 g(r)$ determines the number of neighboring atoms $n(r)dr$ in a spherical shell of radius r and thickness dr centered on a particular atom of interest. The average nearest-neighbor distance a is given by the position of the first peak in $n(r)$, whereas the average coordination number is determined by the area under this peak. Because there is usually considerable overlap between the first- and second-neighbor peaks, experimental values of z depend quite sensitively on the method employed to define and integrate the first neighbor peak.[21] Uncertainties in z of ±2 atoms are common as a result of this ambiguity. Variations of z, say as a function of temperature, can be determined with more reliability as long as a consistent definition of the coordination number is used.

Structural data for expanded liquid metals, and for Hg in particular, are very limited. A number of liquid metals with high boiling points has been investigated over relatively wide ranges of temperature (Rb,[35] Cs,[35] Sn,[36,37] Cd,[37] In,[38] Ga,[37,39]). However, the density reductions achieved in these experiments were less than 10%. An interesting feature of these data is the fact that the positions of the main peak in $S(k)$ and $g(r)$ remain virtually unchanged over the ranges investigated whereas the value of z tends to decrease with the density. There is some evidence, in fact, for a slight *decrease* in a at higher temperatures.[38] In the case of liquid Hg, x-ray measurements over the density range 13.68–12.87 g/cm^3 indicate a constant value $a = 3.07$ Å.[19,20]

The only monatomic liquids whose structures have been investigated over wide ranges of density are the rare-gas liquids. Argon, in particular, has been investigated over the full range from triple point to the region of the critical point.[21] Remarkably, a remains virtually constant while z decreases from about 10 near the triple point to roughly 4 at the critical point. Of course, as we have said, the absolute values of z are rather uncertain but the qualitative behavior is quite clear. Less-complete data for Ne (Ref. 40) are similar although a slight (2.5%) increase in a was re-

ported for a mean density variation of about a factor of 2. The reported values of z drop from roughly 8 to 4 over this range.

Recently, neutron measurements of $S(k)$ for Rb have been reported for densities down to about 70% of the triple point density ρ_t.[41] These data cover only a limited range of k values around the principal maximum and are insufficient for Fourier transformation to obtain $g(r)$. The position of the peak in $S(k)$ is constant down to $\rho \simeq 0.9\,\rho_t$, then shifts toward lower k values by a few percent at the lowest density obtained. This suggests indirectly that a increases somewhat more in Rb than in the rare-gas liquids, but the change is much less than required for uniform expansion at constant z.

In selecting a structural model for liquid Hg we have assumed $a = 3.07$ Å over the entire liquid range. In addition to the advantage of simplicity, this assumption has the rationale that Hg becomes *insulating* well above the critical density and therefore might be expected to resemble the rare-gas liquids at low densities. In this respect Hg differs from Rb which is monovalent and (if it behaves like other alkali metals[42]) transforms to an insulating state only in the near vicinity of the critical point. The present model might be elaborated by allowing some increase in a at low densities. However, we take the point of view that the dominant effect of density reduction on the electronic properties derives from the reduced average coordination number rather than an increased near-neighbor separation.

The simplest structural model with constant a is one in which vacancies are introduced randomly on a close-packed lattice. Furukawa[43] has described such a model for normal high-density liquid metals based on an fcc lattice. This expression for the average coordination number

$$z = 6\sqrt{2}\, n_0 a^3 \qquad (2)$$

yields $z = 10$ for Hg at the melting point, in agreement with most measurements.[19] If we assume that a is constant and that z remains linearly related to the density in the expanded liquid, we find from Eq. (2) that $z = 4$ near the critical density ($\rho_c \approx 5.5$ g/cm^3). Thus, the predicted coordination number at the critical point is the same as observed for liquid Ar, and our extension of Eq. (2) to low densities is consistent with the assumption that Hg and Ar have similar structures near the critical point.

B. Density of states and Knight shift

Our calculated values of $N(E_F)$ can be combined with the simple structural model described above to yield the variation of $N(E_F)$ with density in expanded liquid mercury. The four crystalline structures we have considered correspond to $z = 12$, 8, 6, and 4. Taking $a = 3.07$ Å in Eq. (2), we find $\rho = 16.3$, 10.9, 8.1, and 5.4 g/cm^3, respectively, for the corresponding liquid densities. The fact that the liquid densities are lower than the crystalline ones for coordination 8, 6, and 4 reflects the loss of long-range order in the liquid. There is no such "density defect" for $z = 12$ since the introduction of disorder in a close-packed crystalline structure must necessarily reduce the mean coordination number.

The variations of $N(E_F)$ and $N_s(E_F)$ with density shown in Fig. 5 were obtained by drawing simple smooth curves through the calculated values for the four crystalline structures. The main features of interest for the present discussion are a sharp drop of $N_s(E_F)$ between 16.3 and 11 g/cm^3 and an essentially constant value in the range 8–11 g/cm^3. It is important to note that the total density of states $N(E_F)$ actually *increases* with decreasing density in the latter range.

The interpolated value of $N(E_F)$ at the melting point is $N(E_F) = 1.70 \pm 0.15$ states/(Ry spin atom). This compares well with the value $N(E_F) = 1.6$ states/(Ry spin atom) calculated by Chan and Ballentine using a nonlocal pseudopotential and the experimental liquid structure factor $S(k)$.[44] Since the melting point falls roughly midway between the densities assigned to the fcc and bcc structures, this agreement represents good evidence for the validity of our interpolation.

A second check on this interpolation in the high-density limit is provided by low-temperature heat-capacity and tunneling data for crystalline Hg.

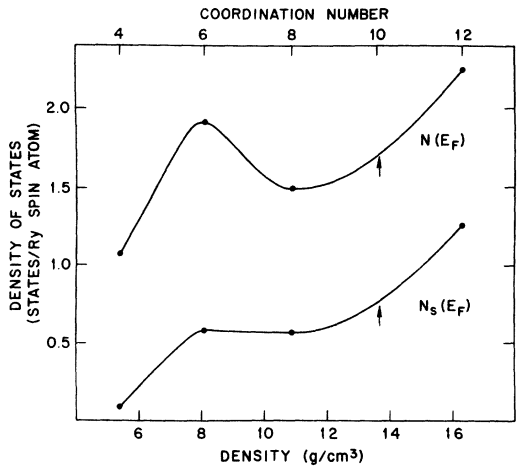

FIG. 5. Interpolated $N(E_F)$ and $N_s(E_F)$ as a function of density (lower scale) and coordination number (upper scale). Densities for four, six, eight, and 12-fold coordination were determined from Eq. (2). Arrows indicate melting point.

McMillan[45] has combined experimental values for the electronic heat-capacity coefficient γ with the observed electron-phonon coupling constant λ to determine the band structure density of states at E_F, $N_{bs}(E_F)$, for rhombohedral Hg ($\rho = 14.5$ g/cm^3). He obtains the value $N_{bs}(E_F) = 1.99$ states/(Ry spin atom), whereas the upper curve in Fig. 5 predicts that $N(E_F) = 1.85$ states/(Ry spin atom) at $\rho = 14.5$ g/cm^3.

The Knight shift is related to the density of states at the Fermi level through the Pauli paramagnetic susceptibility:

$$K = \tfrac{8}{3}\pi \langle |\psi(0)|^2 \rangle_F \chi_a \,, \tag{3}$$

where $\langle |\psi(0)|^2 \rangle_F$ is the probability amplitude at the nucleus averaged over all states at the Fermi level and χ_a is the electron spin susceptibility per atom. Since $|\psi(0)|^2$ is nonvanishing only for states having s character it is convenient to restrict the average in Eq. (3) to s states and to replace χ_a by its s component. Explicitly

$$K = \tfrac{16}{3}\pi \langle |\psi(0)|^2 \rangle_{F,s} \frac{\mu_B^2 N_s(E_F)}{1-\alpha} \,, \tag{4}$$

in which μ_B is the Bohr magneton and $(1-\alpha)^{-1}$ describes the enhancement effects of electron-electron interactions. There are, in general, additional contributions to the Knight shift due to p-electron core-polarization effects and orbital paramagnetism. However, these are expected to be substantially smaller than the s-electron term in s-p band metals. For purposes of the present discussion we can safely neglect these additional contributions.

It is of interest to estimate K using Eq. (4) and our calculated $N_s(E_F)$. To do this we must estimate $\langle |\psi(0)|^2 \rangle_{F,s}$ and $(1-\alpha)^{-1}$. As a rough approximation we take the atomic value $|\psi(0)|^2 = 3.5 \times 10^{26}$ cm^{-3} determined from optical hyperfine measurements[46] on the $^2S_{1/2}$ state in Hg. Use of the atomic hyperfine coupling tends to overestimate $\langle |\psi(0)|^2 \rangle_{F,s}$ since the wave function should spread out more in the metallic state.[47] The value of $(1-\alpha)^{-1}$ can be estimated from the Korringa relation between the shift and the ^{199}Hg spin-lattice relaxation rate T_1: $K^2 T_1 T K(\alpha) = (\hbar/4\pi k_B)(\gamma_e/\gamma_{Hg})^2$ in which γ_e and γ_{Hg} are, respectively, the electronic and nuclear gyromagnetic ratios.[48,49] The correction factor $K(\alpha)$ has been calculated for a free-electron gas[50,51] and thus the experimental value[52] $K(\alpha) = 0.69$ may be used to obtain $(1-\alpha)^{-1} \simeq 1.7$ for Hg. This is a typical value for simple metals. The value of $N_s(E_F)$ at the melting point obtained by interpolation in Fig. 5, $N_s(E_F) = 0.75 \pm 0.05$ states/(Ry spin atom), then yields $K = 2.91\%$. This is to be compared with $K_{expt} = 2.72\%$. The agreement is very good considering the approximations involved and may, in fact, be fortuitous. Nevertheless it is gratifying that the calculated value is somewhat larger than the experimental one, as we anticipated from our use of an atomic hyperfine coupling, and the result lends further support to the interpolation used for obtaining $N_s(E_F)$ at an arbitrary density.

The density dependence of $N_s(E_F)$ is compared with the experimental Knight shift values in Fig. 6. The interpolated curve was normalized to the experimental data at the melting point. It can be seen that $N_s(E_F)$ and K exhibit essentially the same density dependences over the range 9–13.6 g/cm^3. In particular the model values of $N_s(E_F)$ reproduce the plateau in the range 9–11 g/cm^3, reflecting the nearly equal values of $N_s(E_F)$ in the sc and bcc structures. At lower densities the model yields a sharp drop of $N_s(E_F)$ but this occurs below 8 g/cm^3, whereas the drop in the experimental data occurs between 9 and 8 g/cm^3. Some possible explanations of the discrepancy will be discussed in Sec. IV C.

The quantitative success of the model calculation in the density range 9–13.6 g/cm^3 is strong evidence that $N_s(E_F)$ is predominantly responsible for the density dependence of the shift. This conclusion is strengthened by the qualitative similarity of the behavior of $N_s(E_F)$ and K over the entire liquid range including a sharp drop at low densities. One cannot exclude contributions from the density dependence of $\langle |\psi(0)|^2 \rangle_{F,s}$ and $(1-\alpha)^{-1}$, of course, but the present result shows that these effects are not essential to an explanation of the

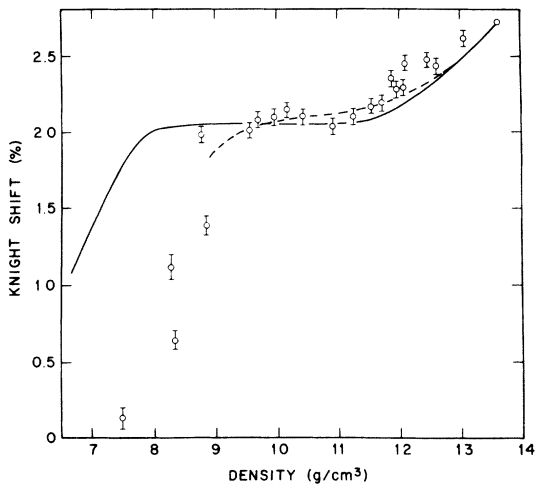

FIG. 6. Experimental (open circles) and calculated Knight shift as a function of density. Solid line: variation of $N_s(E_F)$, normalized to data at $\rho = 13.6$ g/cm^3. Broken line: normalized $N_s(E_F)$ averaged over density fluctuations for sampling volume containing 20 atom volumes.

data. Finally we point out that the constant shift in the range 11–9 g/cm³ does not reflect a compensating rise in fractional s-character at the Fermi level as the total density of states decreases, as required by the "strong-scattering" theory. On the contrary, the results of Table II show that the fraction of s character at the Fermi level actually decreases from 0.37 to 0.30 as the density drops from 11 to 9 g/cm³.

C. Refinements of the model

We consider now two important effects which have been neglected in the simple model described so far. The first of these, obviously, is the possible increase in a at low densities. The second is the increasing importance of density fluctuations as the critical region is approached. It is necessary to estimate the consequences of these effects in regard to conclusions drawn from the model in its simplest form.

1. Variation of the near-neighbor distance

It is clear from the calculations that the value of $N(E_F)$ is extremely sensitive to changes in a in the low-density region. As we have seen, only a 1% increase is required to eliminate the band overlap in tetrahedral coordination. The fact that Hg exhibits semiconducting transport properties for $\rho < 8$ g/cm³ (Refs. 1 and 2) is evidence that a does in fact increase somewhat in this range. A modest increase in a would also tend to shift the sharp drop in $N_s(E_F)$ to higher densities in better accord with experiment. It is likely in fact that one could fit the model calculation to the Knight-shift data by allowing a to be a free parameter. However this would not be very convincing, in the absence of independent structural data, and would require extensive computations. Furthermore, it is possible that part of the discrepancy simply results from errors in density values due to experimental errors in the available data for the equation of state of Hg at low densities.

In addition to circumstantial evidence drawn from the model there is reason to expect that a *should* change in the region of the metal-nonmetal transition. In this region there should occur a change in the pair potential from one characteristic of ions in a metal to one describing the interaction of two neutral Hg atoms. Since the value of the mean interparticle separation in a liquid should be determined mainly by the pair potential, one should expect a change in a at the electronic transition. That the interparticle separation in the Hg_2 molecule is about 3.2 Å can be taken as evidence for this.[53] An increase in a of roughly this magnitude (~4%) would be consistent with the experimental data and, as we have said, would improve the agreement between experiment and theory.

2. Density fluctuations

The effects of density fluctuations in liquid Hg have been much discussed, particularly by Cohen and Jortner.[8] These authors attribute the metal to nonmetal transformation below 9 g/cm³ to a percolation transition in a microscopically inhomogeneous medium. The present band model shows, however, that at least the Knight-shift behavior can be understood without introduction of microscopic inhomogeneity. On the other hand, it is clear on general thermodynamic grounds that density fluctuations are present and become increasingly important as the density decreases. It is therefore of interest to consider the incorporation of density fluctuations into our model.

The Knight shift is a highly local property depending on the average magnetic field experienced by individual nuclei. The shift is relatively insensitive to long-range structural properties, being primarily determined by the local density of conduction electrons. If we consider the liquid divided into an ensemble of small volumes V whose densities are distributed according to a probability distribution $P_v(\rho)$, the average (observed) shift may be written

$$\overline{K} = \int_0^{\rho_{\max}} K(\rho)\rho P_v(\rho)\,d\rho \Big/ \int_0^{\rho_{\max}} \rho P_v(\rho)\,d\rho\,, \qquad (5)$$

where $\rho_{\max}$ is the maximum density possible in the system. For Hg we should take $\rho_{\max} = 16.3$ g/cm³ corresponding to the ideal close-packed structure (fcc). The appearance of a factor ρ in the integrands of Eq. (5) accounts for the fact that the contributions of different regions to the intensity of the NMR signal depend on the number of nuclei present in each region.

In order to test the effect of fluctuations on $\overline{K}$ we use the Gaussian approximation for $P_v(\rho)$ (Ref. 54):

$$P_v(\rho) = (2\pi\xi^2)^{-1/2} \exp(-\gamma^2/2\xi^2)\,, \qquad (6)$$

$$\xi^2 = kT\chi_T/V\,, \quad \gamma = (\rho - \overline{\rho})/\overline{\rho}\,,$$

where χ_T is the isothermal compressibility and $\overline{\rho}$ is the mean density. Values of χ_T can be derived from the available PVT data for Hg.[55] The variation of $\overline{K}$ with $\overline{\rho}$ is shown in Fig. 6 for $V = 4.1 \times 10^{-22}$ cm³ and with $K(\rho)$ given by the interpolation of the calculated values of $N_s(E_F)$. This choice of sampling volume V contains 20 atomic volumes of the fcc crystal and is about the minimum size for which a local Knight shift $K(\rho)$ is meaningful. A larger choice of V, of course, leads to a narrower

distribution $P_v(\rho)$ and hence reduces the effects of fluctuations.

The results of numerical integration of Eq. (5) are compared with the data and with the original version of the model in Fig. 6. As should be expected, the fluctuations are negligible at high densities but begin to introduce noticeable modifications below $\rho \sim 12$ g/cm^3. The overall effect is a slight improvement of the agreement of the model with experiment. Extension of the calculation to densities less than 9 g/cm^3 was considered unreliable because of large uncertainties in the value of χ_T at low densities. In summary we find that inclusion of density fluctuations, at least in the simple form of Eq. (6), does not drastically affect the essential features of our model for densities above 9 g/cm^3. The situation at lower densities remains unclear.

V. DISCUSSION

One of the more interesting features of the energy-band results shown in Fig. 2 is the dependence of the Hg 6s and 6p bandwidths and their overlap on the nearest-neighbor coordination number. It is found, for example, that the 6s bandwidth Δ_s increases systematically from 0.54 Ry for the diamond structure [where $\Delta_s \equiv E(\Gamma_{2'}) - E(\Gamma_1)$] to 0.80 and 0.91 Ry for the sc [$\Delta_s \equiv E(R_1) - E(\Gamma_1)$] and bcc [$\Delta_s \equiv E(H_1) - E(\Gamma_1)$] structures, respectively. This trend is apparently interrupted in the fcc structure, where the 6s bandwidth [$\Delta_s \equiv E(X_1) - E(\Gamma_1)$] is approximately 0.78 Ry.

The present LCAO model provides a simple explanation for this phenomenon. In the case of the diamond, sc, and bcc structures, the 6s bandwidth is determined by the energy difference between states that are fully bonding (Γ_1) and those that are fully antibonding ($\Gamma_{2'}, R_1, H_1$, respectively) with respect to nearest-neighbor interactions. It turns out that a fully antibonding state is incompatible with the translational symmetry of the fcc lattice; this limits the 6s bandwidth to $\frac{2}{3}$ the maximum value (~1.2 Ry) that could be attained in a disordered system.

Similar trends are found in the variation of the Hg 6p bandwidth Δ_p with coordination. In this case, Δ_p depends more critically on the geometrical distribution of nearest neighbors because of the directional bonding characteristics of the p_x, p_y, and p_z orbitals. As a result, larger changes are likely in the energy distribution of p-type states in the liquid.

The present LCAO model predicts that 6s-6p hybridization is approximately independent of coordination in these hypothetical crystalline forms of Hg. The integrals of the 6s component of the density of states N_s in Figs. 4(a)–4(d) predict that the occupied bands in Figs. 2(a)–2(d) contain 71%, 78%, 82%, and 76% 6s character, respectively. It is reasonable to expect that the same degree of 6s-6p hybridization would persist in the liquid state, at least within the density range of 8–14 g/cm^3. This predominance of 6s character in the occupied bands of Hg is clearly the result of the strong relativistic effects which lower the top of the 6s band ($\Gamma_{2'}$) by about 0.25 Ry in Fig. 3(b) relative to the nonrelativistic bands of Fig. 3(a).

The relatively constant degree of s character in the totality of occupied states clearly does not apply to states just at the Fermi level. Here the fractional s character f_s is found to decrease monotonically from 56% to 8% on passing from the fcc to diamond structures. This trend is opposite to that required to reconcile the Knight shift and the strong-scattering transport model. For example, Cohen and Jortner[56] have shown recently that the strong-scattering model requires the product $f_s \langle |\psi(0)|^2 \rangle_{F,s} (1-\alpha)^{-1}$ to increase by roughly a factor of 2 between 11 and 9 g/cm^3. Moreover, they assumed that the liquid expands uniformly ($a \propto \bar{\rho}^{-1/3}$) so that variation of the transfer integral J contributes to the density dependence of the transport coefficients. If the density dependence of a is much weaker than $\bar{\rho}^{-1/3}$, as we have argued elsewhere in this paper, then an even stronger increase in $f_s \langle |\psi(0)|^2 \rangle_{F,s} (1-\alpha)^{-1}$ is necessary. We have no reason to suspect that $\langle |\psi(0)|^2 \rangle_{F,s} (1-\alpha)^{-1}$ should be strongly density dependent in this range and we find from our model calculation that the density dependences of f_s and $N(E_F)$ are in directions opposite to those required by the interpretation of Cohen and Jortner.

It appears, therefore, that there is as yet no adequate theory for describing the electronic transport properties of Hg over wide ranges of density. For the highest densities where $\sigma \gtrsim 3000$ $(\Omega\,\mathrm{cm})^{-1}$ the mean free path is sufficiently long that the Ziman theory for nearly-free-electron liquid metals should apply.[57,58] Once out of this range, as we have seen, there are serious difficulties. One effect which must become important sufficiently close to the critical region is the presence of density fluctuations. Even the simplest Gaussian approximation of Eq. (6) implies a wide distribution of local densities when the mean density is less than about 10 g/cm^3. It is still an open question, however, whether the semiclassical percolation approach of Cohen and Jortner is an adequate way to take these fluctuations into account.

Another type of microscopic inhomogeneity may also contribute to the decreasing conductivity. As the coordination number decreases, the Fermi level in Fig. 2 is systematically lowered relative

to the average interstitial potential. This can be expected to lower the mobility of electrons in these regions. In addition, of course, the interstitial volume represents an increasing fraction of the total volume as the coordination number decreases. Thus, even if the total density of states per atom is roughly constant, there may be a substantial reduction of the conductivity due to this kind of "excluded-volume" effect.

VI. SUMMARY AND CONCLUSIONS

We have presented a model for the electronic structure of expanded liquid mercury based on APW band-structure calculations for hypothetical forms of crystalline Hg. The intent of the study was to investigate the effect on the electronic structure of a decreasing coordination number as Hg expands with constant near-neighbor distance. Available structure data on liquid metals and rare gases suggest that this is a reasonable though somewhat oversimplified representation of the local atomic arrangement. The energy bands and density of states were calculated for the diamond, sc, bcc, and fcc structures using a constant near-neighbor distance given by the position of the first peak in the experimental pair-distribution function. The total density of states for each case was further decomposed into s- and p-electron components. The results showed a gradual development of the $6s$-$6p$ energy gap as the coordination number was reduced, although it was found necessary to increase the lattice constant by 1% to open fully a gap in tetrahedral coordination.

The calculated values for the s component of the density of states at E_F were used to calculate the magnitude and density dependence of the Knight shift; both are in reasonable agreement with experiment. A continuous dependence of the density of states on density was obtained by interpolating values calculated for each of the four crystal structures. A simple vacancy model in which the coordination number depends linearly on density was used to relate each crystal structure to specific liquid density values. The model reproduces a region of constant Knight shift in the range $9 \lesssim \rho \lesssim 11$ g/cm^3 in agreement with experiment. Both experiment and the model exhibit a rapid decrease in shift at lower densities but the predicted density at which this occurs is somewhat below that observed experimentally. This is likely to be a consequence of a small increase in the near-neighbor distance at low densities. The effects of density fluctuations were investigated using a simple theory for $\rho \gtrsim 9$ g/cm^3. Inclusion of fluctuations led to relatively small changes in the predicted density dependence of the Knight shift, but these were in the direction of improved agreement with experiment.

We conclude that a simple quasicrystalline band model represents a reasonable approximation of the electronic structure of expanded liquid Hg. Our results support the hypothesis that a decreasing coordination number is the major influence on the electronic structure as the density decreases. The Knight shift, in turn, is affected mainly by variations in the s component of the density of states. The calculations show, however, that the s and p components of the density of states exhibit different density dependences and that one cannot, therefore, infer the behavior of the total density of states from that of the Knight shift. On the other hand, these differences are in the wrong sense to reconcile the apparent inconsistency of the Knight shift and electronic transport properties. As a result there remain serious difficulties with the available theory of electronic transport in liquid Hg in the range between the domain of nearly-free-electron theory and the metal-nonmetal transition.

ACKNOWLEDGMENTS

We wish to thank J. H. Wood for providing the Dirac-Hartree-Fock-Slater atomic charge density for mercury that has been used in this investigation. We are grateful to A. C. Switendick for providing various program listings and input data that were useful in setting up an APW program for the diamond structure. We are indebted to F. Hensel for helpful and stimulating discussions of this work.

[1]E. U. Franck and F. Hensel, Phys. Rev. 147, 109 (1966); F. Hensel and E. U. Franck, Rev. Mod. Phys. 40, 697 (1968).
[2]R. W. Schmutzler and F. Hensel, Phys. Lett. A 35, 55 (1971); Ber. Bunsenges. Phys. Chem. 76, 531 (1972).
[3]L. J. Duckers and R. G. Ross, Phys. Lett. A 38, 291 (1972).
[4]U. Even and J. Jortner, Phys. Rev. Lett. 28, 31 (1972); Philos. Mag. 25, 715 (1972); Phys. Rev. B 8, 2536 (1973).
[5]U. El-Hanany and W. W. Warren, Jr., Phys. Rev. Lett. 34, 1276 (1975).
[6]N. F. Mott, Philos. Mag. 13, 989 (1966); Adv. Phys. 16, 49 (1967); Philos. Mag. 26, 505 (1972).
[7]N. F. Mott, Philos. Mag. 19, 835 (1969).
[8]M. H. Cohen and J. Jortner, Phys. Rev. Lett. 30, 699 (1973); Phys. Rev. A 10, 978 (1974).
[9]M. H. Cohen, J. Non-Cryst. Solids 4, 391 (1970).

[10]N. F. Mott, Philos. Mag. 24, 1 (1971).
[11]N. K. Hindley, J. Non-Cryst. Solids 5, 17 (1970).
[12]L. Friedman, J. Non-Cryst. Solids 6, 329 (1971); Philos. Mag. 28, 145 (1973).
[13]Y. Baer and H. P. Myers, Solid State Commun. 21, 833 (1977).
[14]M. A. C. Devillers and R. G. Ross, J. Phys. F 5, 73 (1975).
[15]H. Overhof, H. Uchtmann, and F. Hensel, J. Phys. F 6, 523 (1976).
[16]P. Fritzson and K.-F. Berggren, Solid State Commun. 19, 385 (1976).
[17]F. Yonezawa and F. Martino, Solid State Commun. 18, 1471 (1976); F. Yonezawa, F. Martino and S. Asano, in *Liquid Metals 1976*, edited by R. Evans and D. A. Greenwood, (Institute of Physics, London, 1977).
[18]H. Uchtmann and F. Hensel, Phys. Lett. A 53, 239 (1975).
[19]Y. Waseda and K. Suzuki, Phys. Status Solidi 40, 183 (1970).
[20]Y. Waseda, K. Yokoyama, and K. Suzuki, Philos. Mag. 29, 1427 (1974).
[21]S. J. Pings, in *Physics in Simple Liquids*, edited by H. N. V. Temperley, J. S. Rowlinson, and G. S. Rushbrooke (North-Holland, Amsterdam, 1968).
[22]J. C. Slater and G. F. Koster, Phys. Rev. 94, 1498 (1954).
[23]D. Liberman, J. T. Waber, and D. T. Cromer, Phys. Rev. 137, A27 (1965).
[24]J. C. Slater, Adv. Quantum Chem. 6, 1 (1972).
[25]P. D. DeCicco, Phys. Rev. 153, 931 (1967).
[26]S. C. Keeton and T. L. Loucks, Phys. Rev. 152, 548 (1966).
[27]F. Herman and S. Skillman, *Atomic Structure Calculations* (Prentice-Hall, Englewood Cliffs, N.J., 1963).
[28]L. F. Mattheiss, Phys. Rev. 151, 450 (1966).
[29]T. Loucks, *Augmented Plane Wave Method* (Benjamin, New York, 1967).
[30]G. Dresselhaus and M. S. Dresselhaus, Phys. Rev. 160, 649 (1967).
[31]I. Alstrup and K. Johansen, Phys. Status Solidi 28, 555 (1968).
[32]L. F. Mattheiss, Phys. Rev. B 5, 290 (1972).
[33]O. Jepson and O. K. Andersen, Solid State Commun. 9, 1763 (1971).
[34]G. Lehmann and M. Taut, Phys. Status Solidi B 54, 469 (1972).
[35]N. S. Ginrich and L. Heaton, J. Chem. Phys. 34, 873 (1961).
[36]K. Furukawa, B. R. Orton, J. Hamor, and G. I. Williams, Philos. Mag. 8, 141 (1963).
[37]C. N. J. Wagner, in *Liquid Metals 1976*, edited by R. Evans and D. A. Greenwood, (Institute of Physics, London, 1977).
[38]H. Ocken and C. N. J. Wagner, Phys. Rev. 149, 122 (1966).
[39]A. S. Lashko and Yu. G. Poltavtsev, Kristallog. 13, 352 (1968) [Sov. Phys.-Crystallogr. 13, 287 (1968)].
[40]P. W. Schmidt and C. W. Tompson, in *Simple Dense Fluids*, edited by H. L. Frisch and Z. W. Salsburg (Academic, New York, 1968).
[41]R. Block, J. B. Suck, W. Freyland, F. Hensel, and W. Glaser, in Ref. 37.
[42]F. Hensel, Angew. Chemie 13, 446 (1974).
[43]K. Furukawa, Sci. Rep. Res. Inst. Tohoku Univ. A12, 368 (1960).
[44]T. Chan and L. E. Ballentine, Phys. Lett. A 35, 385 (1971).
[45]W. L. McMillan, Phys. Rev. 167, 331 (1968).
[46]S. Mrozowski, Phys. Rev. 57, 207 (1940).
[47]W. Knight, in *Solid State Physics*, edited by F. Seitz and D. Turnbull (Academic, New York, 1956), Vol. 2.
[48]T. Moriya, J. Phys. Soc. Jpn. 18, 516 (1963).
[49]A. Narath and H. T. Weaver, Phys. Rev. 175, 373 (1968).
[50]R. W. Shaw, Jr. and W. W. Warren, Jr., Phys. Rev. B 3, 1562 (1971).
[51]P. Bhattacharyya, K. N. Pathak, and K. S. Singwi, Phys. Rev. B 3, 1568 (1971).
[52]D. A. Cornell, Phys. Rev. 153, 208 (1967).
[53]J. G. Winans and M. P. Heitz, Z. Phys. 133, 291 (1952); 135, 406 (1953).
[54]L. D. Landau and E. M. Lifshitz, *Statistical Physics* (Pergamon, London, 1958), p. 351.
[55]F. Hensel and E. U. Franck, Ber. Bunsenges. Phys. Chem. 70, 1154 (1966); I. Kikoin and A. R. Sechenkov, Fiz. Metallov. Metaloved. 24, 843 (1967) [Phys. Metals. Metallogr. (U.S.S.R.) 24, 74 (1967)]; D. R. Posthill, R. G. Ross, and N. E. Cusack, Philos. Mag. 18, 519 (1968).
[56]M. H. Cohen and J. Jortner, Phys. Rev. B 15, 1227 (1977).
[57]J. M. Ziman, Philos. Mag. 6, 1013 (1961).
[58]R. Evans, D. A. Greenwood, P. Lloyd, and J. M. Ziman, Phys. Lett. A 30, 313 (1969); R. Evans, J. Phys. C. Suppl. 2, S137 (1970).